Soft Matter

Accepted Manuscript

This article can be cited before page numbers have been issued, to do this please use: C. M. O. Lepori, N. M. M. CORREA, J. J. Silber and R. D. Falcone, *Soft Matter*, 2015, DOI: 10.1039/C5SM02421H.

ROYAL SOCIETY OF CHEMISTRY

www.rsc.org/softmatter

View Article Online
DOI: 10.1039/C5SM02421H

How the Cation 1-butyl-3-methylimidazolium Impacts on the Interaction between the Entrapped Water and the Reverse Micelles Interface Created with an Ionic Liquid-like Surfactant

Cristian M. O. Lépori, N. Mariano Correa, Juana J. Silber, R. Darío Falcone*[a]

[a] Lic. C. M. O. Lépori, Prof. N. M. Correa, Prof. J. J. Silber and Dr. R. D. Falcone.

Departamento de Química. Universidad Nacional de Río Cuarto. Agencia Postal # 3. C.P. X5804BYA Río Cuarto. ARGENTINA.

* Corresponding-Author: Dr. R. Darío Falcone. E-mail: rfalcone@exa.unrc.edu.ar

View Article Online
DOI: 10.1039/C5SM02421H

ABSTRACT

The behavior of the interfacial water entrapped in reverse micelles (RMs) formed by the ionic liquid-like surfactant: 1-butyl-3-methylimidazolium 1,4-bis-2-ethylhexylsulfosuccinate (bmim-AOT) dissolved in benzene (or chlorobenzene) was investigated using noninvasive techniques such as dynamic (DLS) and static (SLS) light scattering, FT-IR and ^{1}H NMR.

DLS and SLS results reveal the formation of discrete spherical and non-interacting water droplets stabilized by the bmim-AOT surfactant. Moreover since the droplet sizes values increase as the W_0 (W_0 = [Water]/[Surfactant]) values increase, water interacts with the RMs interface.

From FT-IR and ^{1}H NMR data, a weaker water-surfactant interaction in bmim-AOT RMs in comparison with the RMs created by sodium 1,4-bis-2-ethylhexylsulfosuccinate (Na-AOT) is detected. Consequently there are less water molecules interacting with the interface in bmim-AOT RMs, and its hydrogen bond network is not completely disrupted as it is in Na-AOT RMs. The results show how the nature of the new cation impact on the interaction between the entrapped water and the RM interface, modifying the interfacial water structure in comparison with the results known for Na-AOT.

View Article Online
DOI: 10.1039/C5SM02421H

INTRODUCTION

Ionic Liquids (ILs) are a new class of compounds which have received significant attention as powerful alternatives to conventional molecular organic solvents.[1] Negligible vapor pressure, combined with excellent chemical and thermal stability, ease of recyclability and widely tunable properties such as polarity, hydrophobicity and solvent miscibility through appropriate modification of the cation and anion, makes ILs neoteric material for a number of chemical processes.[1] Most ILs used are based on *N*,*N*′-dialkylimidazolium cations, especially 1-butyl-3-methylimidazolium ($bmim^+$, Scheme 1) and different anions such as tetrafluoroborate (BF_4), hexafluorophosphate and bis(trifluoromethylsulfonyl)imide.[1] The great impact that ILs actually have is mainly because their properties can be modified by a variety of cation-anion combinations in the synthesis procedure. Principally, this provides an attractive and emerging field where amphiphilic ILs have been synthesized.[2] These *IL-like surfactants* can be used to create different kind of molecular assemblies such as direct micelles, reverse micelles (RMs) and vesicles.[2-9]

RMs are a kind of organized system, generally described as nanometer sized water droplets dispersed in a nonpolar solvent with the aid of a surfactant monolayer, forming a thermodynamically stable and optically transparent solution.[10,11] Different anionic, cationic and nonionic surfactants have been employed to prepare RMs in nonpolar solvents.[10] Among the anionic surfactants that form RMs in different solvents, the best known is the sodium 1,4-bis-2-ethylhexylsulfosuccinate (Na-AOT).[10-13] It is known that Na-AOT forms spherical RMs in aromatic and aliphatic solvents without addition of a cosurfactant and, variable amount of water can be solubilized depending on the external solvent and temperature.[12]

The majority of studies on RMs solubilize water as the polar component and juxtapose water properties such as polarity, viscosity, conductivity and H-bonding for bulk water and water confined in RMs.[14-32] These studies show that the physicochemical properties of water entrapped inside RMs change dramatically from the bulk, as a result of the specific interactions and confined geometries.[10,22,27,31] Moreover, it has been demonstrated that the effect of the kind of surfactant used

View Article Online
DOI: 10.1039/C5SM02421H

to create RMs is crucial for the understanding of the water structure.[17,18,20,23] Previous studies performed in our group have shown very peculiar and interesting water properties inside RMs that emerges from the confinement effect and the interaction with the surfactant at the interface.[17,18,20,23] For example, water properties differ between RMs systems formed with anionic and cationic surfactants. The water molecules entrapped inside Na-AOT RMs show enhanced electron donor ability compared with bulk water, while water entrapped inside benzyl-n-hexadecyldimethylammonium chloride RMs appears non electron-donating due to its interaction with the cationic surfactant polar headgroup.[17,18,20] These results have tremendous impact when RMs are used as nanoreactors.[18,33,34]

Alterations on the RMs properties also have been obtained in the past, replacing Na^+ counterion in the Na-AOT surfactant by different inorganic counterions such as alkali metals among others.[12,26,29,35-45] For example, Eastoe et al.[40] showed effect on the form of the aggregates using Na^+, K^+, Rb^+, Cs^+, Mg^{2+}, Ca^{2+}, Co^{2+}, Ni^{2+}, Cu^{2+}, Zn^{2+}, and Cd^{2+} as counterions of AOT in cyclohexane. The authors invoked the importance of the size of the hydrated counterion on the aggregate structure (spherical and cylinder-shaped aggregates) in RMs. Thus, a large hydrated counterion cannot no be located near to the SO_3^- headgroups as effectively as a small ion like Na^+. This fact alters the surface curvature of the aggregate due to the impact of the electrostatic repulsive interactions between adjacent polar headgroups.

On the other hands, recent studies on RMs with an IL component have garnered interest because of the ILs can act as surfactant, as external medium or as internal polar pseudophase.[46] Particularly, several authors have performed the replacement of the Na^+ counterion in Na-AOT by organic cations such as tetraalkylammonium[47-49] or $bmim^+$ (bmim-AOT, Scheme 1)[50-54] in order to create ionic-liquid surfactants that generated very different properties compared with the precursor Na-AOT. These AOT analogues (most of them room temperature ILs), have been used mainly to create direct micelles in water[50-52,54,55] and RMs prepared in nonpolar solvents entrapping other ILs as polar component.[56-,,,60] For example, Rao et al.[56-60] have characterized the phase diagram of the

View Article Online
DOI: 10.1039/C5SM02421H

$bmimBF_4$/bmim-AOT/benzene ternary system by dynamic light scattering (DLS) and spectroscopic studies with various molecular probes.[56] Bai et al.[53] have explored the same RMs by mixing the IL with water and they found that the droplet sizes values depend on the amount of water and $bmimBF_4$ content. Surprisingly, no studies about the ability of the new surfactant bmim-AOT to create RMs entrapping only water (aqueous RMs) are available. Particularly, this motivates us to explore how is the interaction between the water entrapped and the interface formed by the AOT surfactant in RMs, where the cationic component (Na^+) is replaced by a larger and more hydrophobic cation. In this sense, we recently have synthesized two ILs-like surfactants (classified as *catanionic surfactants*[61]) but in contrast to bmim-AOT, they are composed by amphiphilic organic cations such as benzyl-n-hexadecyldimethylammonium and cetyltrimethylammonium.[4,5] Both ILs were able to form RMs and the encapsulated water properties depend on the cationic component at the RMs interface.[4,5]

In this contribution we have investigated, by different noninvasive techniques such as DLS and static light scattering (SLS), FT-IR and ^1H NMR spectroscopies, the ability of bmim-AOT to form aqueous RMs in nonpolar solvents and how the nature of the new cation impacts on the interaction between the entrapped water and the RM interface, modifying the interfacial water structure in comparison with the results known for Na-AOT. In this sense, understanding the structure of water entrapped in RMs is of great importance in many contexts, including for example dehydration of biological molecules,[62,63] enzyme activity[18], water entrapped in nanopores materials,[64] nanoparticles synthesis[34,65] among other.

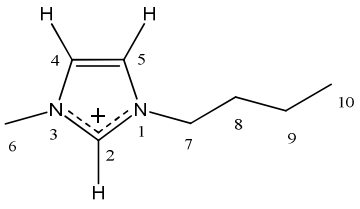

bmim$^+$

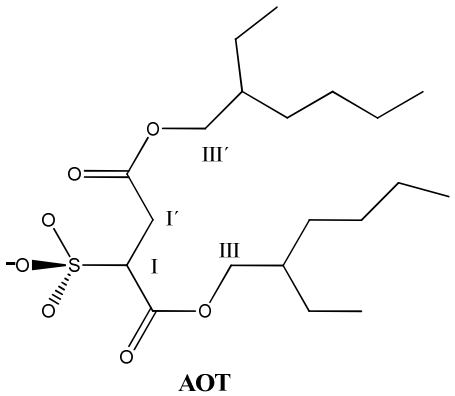

AOT

View Article Online
DOI: 10.1039/C5SM02421H

Scheme 1. Molecular structure of the surfactant bmim-AOT. Specific protons observed in the NMR spectra are identified.

RESULTS AND DISCUSSION

I. Solubilization of bmim-AOT in nonpolar solvents

In order to evaluate if the IL bmim-AOT can be used as surfactant to generate RMs, the first experiment performed was to investigate the phase diagram of the ternary system: water/surfactant/nonpolar solvent. As it was described above, there are only few reports about the use of bmim-AOT as surfactant dissolved in nonpolar solvent, mainly in benzene.[53,57,60] Thus, the bmim-AOT solubility in different nonpolar solvents was tested. Therefore, the bmim-AOT solubility in nonpolar solvents commonly used to formulate RMs[10,11] such as chlorobenzene, toluene and *n*-heptane, was investigated. It was observed that bmim-AOT is soluble in all aromatic solvents in absence of water (W_0 (W_0 = [Water] / [Surfactant]) = 0). However, in *n*-heptane bmim-AOT was completely insoluble. It must be noted that bmimCl, which is the IL precursor of the $bmim^+$ cation of the surfactant (See experimental section), is a molecule without amphiphilic property that cannot be dissolved in either nonpolar aromatic or aliphatic solvents[1] but the precursor surfactant, Na-AOT, is fully soluble in both kind of solvents.[10] Thus, the solubility of AOT moiety is clearly altered by presence of the organic cationic component ($bmim^+$).

II. Non-polar aromatic solvents/bmim-AOT solutions as systems to dissolve water

The amount of water that can be dispersed in the nonpolar solvent/bmim-AOT solutions forming clear and stable ternary mixtures is summarized in Table 1, for [bmim-AOT] = 0.1 M. The maximum amount of water solubilized in the different bmim-AOT systems is defined as W_0^{max}. For comparison, in Table 1 are also included the Na-AOT systems prepared in all the nonpolar solvents evaluated. As it can be observed, the W_0^{max} values reached for the aromatic solvents/bmim-AOT systems are quite similar. All of them are able to dissolve approximately the half amount of water

View Article Online
DOI: 10.1039/C5SM02421H

than the corresponding Na-AOT systems.[10] These results show that bmim-AOT IL-surfactant when dissolved in aromatic solvents it has the ability to dissolve water. Thus, it is interesting to investigate if the presence of the $bmim^+$ cation in bmim-AOT (See Scheme 1) produces different physicochemical properties in comparison with Na-AOT such as hydrogen bond and electron donor ability of the interface, among others.

Table 1. Maximum amount of water solubilized (W_0^{max}) in different systems at [surfactant] = 0.1 M. T = 25 ºC.

Non-polar solvent	W_0^{max}	
	bmim-AOT	Na-AOT
n-heptane	-[a]	60[b]
benzene	5.0	12[b]
chlorobenzene	5.4	8[c]
toluene	5.1	10[d]

[a] bmim-AOT is not soluble in *n*-heptane. [b] Value obtained from reference 34. [c] Value obtained from reference 66. [d] Value obtained from reference 67.

III. DLS and SLS experiments

To evaluate the formation of RMs[11,24] the system formed by benzene/bmim-AOT/water was studied by DLS technique.

When new RMs are explored, a crucial question has to be answered: is water effectively entrapped by the surfactant creating a true RMs or is water dissolved only in the organic solvent/surfactant mixture without any molecular organization (bicontinous structureless microemulsion)?.[24] DLS can be used to assess this matter because if water is really encapsulated and interacting with the RM interface, the droplets size must increase as the W_0 value increases with a linear tendency (swelling law of RMs) as it is well established for other RMs.[21,46,68] This

View Article Online
DOI: 10.1039/C5SM02421H

feature can also demonstrate that the RMs consist of discrete spherical and non-interacting droplets.[21] A deviation from the linearity on the droplets sizes indicates that the RMs droplet – droplet interactions are favored thus changing the shape of the RMs previous to the phase separation. On the other hand, if the polar solvent is not encapsulated by the surfactant the droplets sizes could remain constants or even decrease with the polar solvent addition.[24]

In this work, all the DLS experiments were carried out at finite surfactant concentration (0.05 M). Thus, the RMs solutions are not at infinite dilution, nevertheless we think that the interdroplet interactions could be neglected.[5,68,69] An apparent hydrodynamic diameter (d_{app}) can be defined,[69,70] in order to make the comparison with the system herein studied and the known Na-AOT systems.[13,34,71] In Figure 1, the d_{app} values for the RMs studied at different W_0 values for bmim-AOT systems are shown. It must be noted that the maximum amount of water that the benzene/bmim-AOT RMs support to yield stable and transparent systems corresponds to $W_0 = 5$. Additionally, in Table S1 (Supporting Information section) are reported the polydispersity index (PDI) values obtained. As it can be seen, there is an increase in the droplet size when the content of water increases, showing that the water is entrapped by the bmim-AOT surfactant layer yielding RMs. Also, the linear tendency observed in Figure 1 and the low PDI values (0.02-0.07) reported in Table S1, confirm that the droplets effectively are not interacting and the shapes are probably spherical[71] and water interacts strongly with the interface. It is important to note that, variations in the droplets sizes (and morphology) changing the surfactant concentration were not observed.

View Article Online
DOI: 10.1039/C5SM02421H

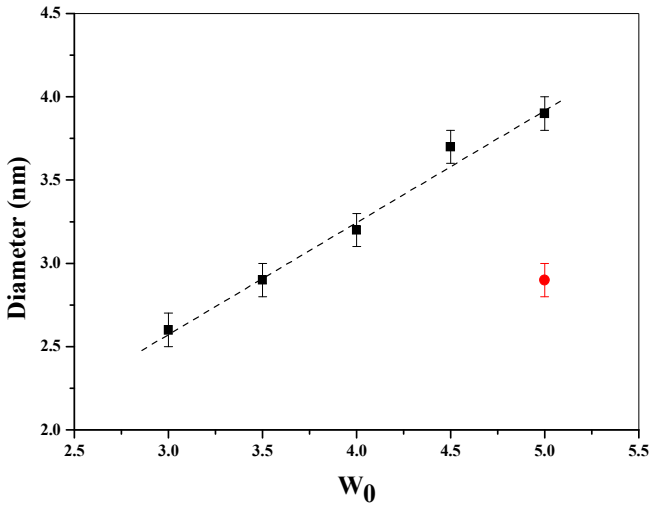

Figure 1. Apparent diameter (d_{app}) values of the (■) benzene/bmim-AOT/water RMs obtained at 25 °C varying W_0. The straight line is plotted to guide the eye. [Surfactant] = 0.05 M. (●) Data for benzene/Na-AOT/water RMs obtained under same conditions.

Even that the W_0^{max} values reached by bmim-AOT in aromatic solvents are not large, it is interesting to remark that it is possible to determine the droplets size values at lower water content than in benzene/Na-AOT RMs. Thus, in benzene/bmim-AOT media it can be detected organized media even at W_0 = 2 while in benzene/Na-AOT the lowest W_0 content detected with our equipment was 5.[34] For this reason and, that the benzene/bmim-AOT system is not able to dissolve more water than W_0 = 5, we only can compare both systems at this water content. Hence, at W_0 = 5 the d_{app} value for bmim-AOT RMs is around 3.9 nm and for Na-AOT RMs is around 2.9 nm.[34] Prior to explain these results it is important to consider that the RMs droplet sizes depend, among many other variables, on the effective packing parameter of the surfactants p, defined as $p = v/al_c$, in which v and l_c are the volume and the length of the hydrocarbon chain, respectively and a is the surfactant head group area.[71] The RMs sizes are larger when the p values are smaller.[72,73] Thus, all the factors that decrease the v values and/or increase the a values decrease the packing parameter affecting the RMs droplet sizes. It has been shown using DLS, that in Na-AOT,[68,74,75] the polar

View Article Online
DOI: 10.1039/C5SM02421H

solvents-surfactant interactions are the key for the RMs droplets sizes control. For example, when a polar solvent encapsulated interacts strongly with the surfactant polar head group increase the surfactants' *a* values with the consequent decrease in the surfactant packing parameter and, the increase in the RM droplet size.[68]

Considering our DLS results, the differences in the droplets sizes of the bmim-AOT RMs in comparison with the corresponding reported by the precursor Na-AOT can be explained as follow: The ionic nature of the polar head group of the precursors (Na-AOT and bmimCl) and the necessity to act as counterion of each other in the new IL-like surfactant, produces a change in the *p* parameter in comparison with the Na-AOT precursor. We hypothesize that due to the replacement of the Na^+ counterion of AOT by $bmim^+$, an increment in the effective area (decreasing the *p* value) of the IL-surfactant can be expected. Thus, in the new interface probably the $bmim^+$ counterion, which is more hydrophobic than Na^+, is located in different region that Na^+ in the Na-AOT RMs.

In order to support the idea that the replacement of Na^+ by $bmim^+$ produces alteration at the interfacial level in the RMs formed, SLS technique was used. The aggregation numbers (N_{agg}), i.e. the number of surfactant molecules per micelle, of bmim-AOT and Na-AOT systems at equal W_0 were determined and, the values are listed in Table 2. As can be seen, at $W_0 = 5$ bmim-AOT RMs present a N_{agg} value similar to that of Na-AOT RMs. Thus, assuming that the Na-AOT RMs are practically spherical,[34,71] and that the bmim-AOT RMs are also spherical as it was assumed by DLS experiments, the variation in the d_{app} values (Figure 1) cannot be attributed to the number of molecules that form the RMs but probably to the location of the $bmim^+$ counterions near the AOT moiety as we will show later. This possible location of $bmim^+$ cation was previously proposed in RMs created by Na-AOT but entrapping the IL 1-butyl-3-methylimidazolium trifluoromethanesulfonate (bmimTfO) as polar component.[75] In that work, we suggested that when bmimTfO is encapsulated in AOT RMs, the cation $bmim^+$ penetrates the interface toward the proximity of the SO_3^- group while the TfO^- anions interact with the Na^+ counterions far from the interface. Thus, the presence of $bmim^+$ at the interface increases the effective interfacial area,

View Article Online
DOI: 10.1039/C5SM02421H

decreases the surfactant packing parameter with the consequent increase in the RMs size. Similarly, Murgia et al.[76,77] proposed that $bmim^+$ tends to be close to the AOT moiety in aqueous Na-AOT direct micelles when 1-butyl-3-methylimidazolium tetrafluoroborate or 1-butyl-3-methylimidazolium bromide is added.

It is must be noted that, the $bmim^+$ location suggested in the present work is different to the one reported by the catanionic surfactants created with benzyl-n-hexadecyldimethylammonium and cetyltrimethylammonium as AOT counterions.[4,5] In that work the cationic components are more hydrophobic and ampliphilic than the $bmim^+$ ion which force them to be located intercalated between the AOT moiety.

Table 2. Aggregation numbers (N_{agg}) for the benzene/bmim-AOT/water and benzene/Na-AOT/water RMs calculated using de SLS technique. T = 25 ºC. W_0 = 5.

RMs	d_{app} (nm)[a]	N_{agg}
benzene/bmim-AOT/water	3.9	23 ± 2
benzene/Na-AOT/water	2.9	17 ± 1

[a] Data from Figure 1.

IV. FT-IR experiments

In order to obtain more insights on the structure of the bmim-AOT RMs, we choose to monitor the microenvironment that the water and the surfactant molecules experiment inside bmim-AOT RMs by FT-IR techniques. Thus, we firstly focus on the O-D stretching mode of the entrapped water molecules and then, on the symmetric and asymmetric S=O, carbonyl stretching modes from the AOT moiety (Scheme 1) and finally the C-H aromatic stretching mode of $bmim^+$ (Scheme 1). The results were compared with the stretching vibration modes of Na-AOT.

O-D stretching band ($\nu_{O\text{-}D}$)

View Article Online
DOI: 10.1039/C5SM02421H

It is well known that water exhibits a broad band in the 3500-3200 cm^{-1} region, which is assigned to the O-H stretching.[78] In liquid phase this band not only corresponds to the O-H stretching but also to coupled water molecule vibrations and from a bending overtones reported in the spectrum of liquid water.[79,80] This is also explains the broad band in the 2570-2350 cm^{-1} region also observed for deuterated water (D_2O). In our FT-IR studies we decided to use monodeuterated water (HDO), which exhibit a narrow band around 2570-2350 cm^{-1} that can be assigned only to the O-D stretching band (ν_{O-D}) with no couplings contributions.[80,81] This methodology was used before in different RMs in order to avoid the vibrational coupling and simplify the data analysis.[5,15,25,26,28,32,81-83]

Figure S1, in the Supporting Information Section, displays the FT-IR spectra of HDO entrapped in bmim-AOT RMs (Figure S1 A) and Na-AOT (Figure S1 B) at different W_0, in the region of 2640-2420 cm^{-1}. From both Figures it is possible to observe that the O-D band is practically symmetrical, suggesting only one type of water entrapped by the RMs.[83] Figure 2 shows the shifts of the ν_{O-D} values for HDO in both RMs and two facts can be observed: i) the O-D stretching frequency values in bmim-AOT RMs are larger than the corresponding to neat HDO (2519 cm^{-1})[84] and, ii) the trend in the changes of the ν_{O-D} values is different between both RMs.

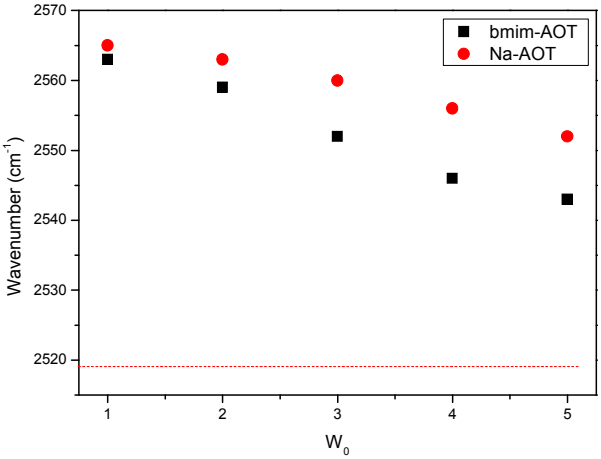

Figure 2. Shifts of the O-D stretching band (ν_{O-D}) upon increases W_0 for the (■) benzene/bmim-

View Article Online
DOI: 10.1039/C5SM02421H

AOT/HDO and (●) benzene/Na-AOT/HDO RMs. The corresponding value for neat HDO (---) is included as a reference.

As it is known for Na-AOT RMs,[80-82] the hydrogen bond interaction between the entrapped water and the SO_3^- group of AOT at the interface disrupt the hydrogen bond network of water, consequently the ν_{O-D} values for HDO appear at larger frequencies than in bulk water. In our case, the fact that the entrapped water in bmim-AOT RMs presents also ν_{O-D} values larger than neat water, suggests that water molecules interact through hydrogen bonding with the surfactant interface breaking its hydrogen bond structure. Additionally, Figure 2 also shows that although in both RMs the ν_{O-D} values shift to lower frequencies as W_0 increases, the changes in magnitude are different. For example, in Na-AOT RMs the frequency of the O-D band change from 2565 cm^{-1} at $W_0 = 1$ up to 2552 cm^{-1} at $W_0 = 5$ (13 cm^{-1}), while in bmim-AOT RMs at the same range of W_0 the ν_{O-D} values shift from 2563 cm^{-1} to 2543 cm^{-1} (20 cm^{-1}). These results suggest a difference in the magnitude of the water-surfactant interaction at the interface. Even though both surfactants display hydrogen bond interaction, the strength of this seems to be different. When the water-surfactant interaction at the RM interface is strong, the water molecules have the hydrogen bond network disrupted and, produce small changes in the ν_{O-D} values varying the water content. On the contrary, if the interaction is weak the water molecules can make hydrogen bond among each other producing a larger shift of the ν_{O-D} values.[5]

Carbonyl stretching band ($\nu_{C=O}$)

In Figure 3 A is plotted the carbonyl stretching band for the Na-AOT and bmim-AOT surfactants dissolved in benzene at $W_0 = 0$. From the Figure it is possible to observe that the C=O band for bmim-AOT surfactant shows a notable difference in its shape in comparison with the one observed for Na-AOT. The carbonyl stretching band of Na-AOT has been widely studied both in solid state[80] and in RMs.[30,83,85-88] It appears as a broad band with a peak around 1736 cm^{-1} and a

View Article Online
DOI: 10.1039/C5SM02421H

shoulder around 1724 cm^{-1}. In this sense, the explanations given for the Na-AOT C=O band shape were quite confusing and the causes of its asymmetry were not clear. However, recently[5,83] we suggested that the Na-AOT C=O band shape can be attributed to the presence of the Na^+ counterion near to one of the carbonyl groups which promotes the asymmetry in the C=O band. Thus, replacing the AOT counterions by different amphiphilic quaternary ammonium[5], the C=O band appears as a symmetrical band with a peak around 1735-1734 cm^{-1}. In the present work, the Na^+ replacement by $bmim^+$ clearly shows that the asymmetry of the carbonyl stretching band is lost as observed with quaternary ammonium ions.[5]

In Figure 3 B is shown the FT-IR spectra in benzene/bmim-AOT/water RMs in the region of C=O stretching mode by varying the amount of water. As it can be seen, the C=O stretching band does not show any significant change in its position (1735 cm^{-1}), shape or absorbance as the value of W_0 is increased. It is known that many factors can influence the position of the C=O band, including hydrogen bond formation and ionic interactions, which lead to displacement of the band to lower frequencies.[80] Additionally, the hydrogen bond interaction not only induces a shift of the band but can produce a marked effect on its intensity. The absorption coefficient of the band increases multiple units when the carbonyl group makes hydrogen bond interaction. Durantini et al.[87] found that in *n*-heptane/Na-AOT/ethylene glycol and *n*-heptane/Na-AOT/propylene glycol RMs, both polar solvents not only interact strongly with the sulfonate group but also penetrate the micelle interface enough to interact through hydrogen bond with the carbonyl groups of the surfactant. This interaction was reflected in a large increase in the intensity of the C=O band. As Figure 3 B shows in bmim-AOT RMs, the lack of absorption changes in the stretching band of carbonyl group of the AOT moiety indicate that the entrapped water does not penetrate the interface enough to interact through hydrogen bonds with the carbonyl groups of AOT.

View Article Online
DOI: 10.1039/C5SM02421H

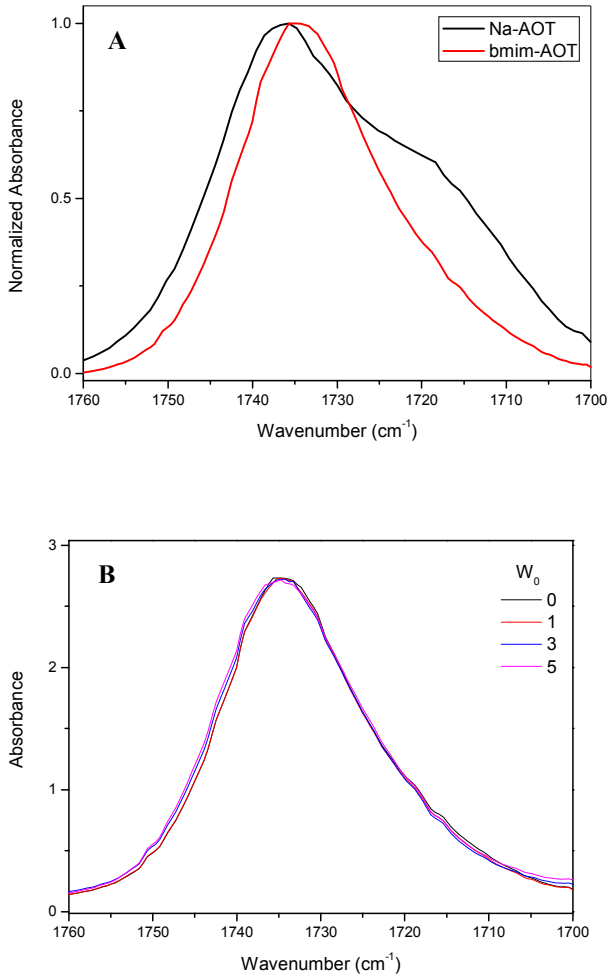

Figure 3. A) Comparison of the normalized FT-IR spectra of benzene/bmim-AOT and benzene/Na-AOT RMs at $W_0 = 0$. B) FT-IR spectra of benzene/bmim-AOT/water RMs at different W_0 values in the region of 1700-1760 cm^{-1}. The benzene bands have been subtracted. [Surfactant] = 0.05 M.

Sulfonate asymmetric stretching band (ν_{asym} SO_3)

The anionic AOT moiety presents two sulfonate stretching vibration modes which are sensitive to different effects: the asymmetric S=O stretching band (around 1130 - 1330 cm^{-1}) and the symmetric S=O stretching mode (around 1050 cm^{-1}).[87,89,90] However, taking into account the strong in-plane C-H bending mode of benzene (around 1060-1020 cm^{-1}), the symmetric S=O stretching mode cannot be observed in RMs prepared in this solvent. For this reason chlorobenzene was used to explore these vibration bands.

View Article Online
DOI: 10.1039/C5SM02421H

The FT-IR band assigned to the asymmetric stretching mode of the sulfonate group ($\nu_{asym}SO_3$) appears as a weak doublet at about 1214 and 1242 cm^{-1} in solid Na-AOT, which has been attributed to the lifting of the degeneracy of this vibration by an asymmetric interaction of the Na^+ with the sulfonate head group.[88b] The magnitude of the splitting, defined as $\Delta\nu_{asym}SO_3$, is indicative of the strength of the perturbation of the SO_3^- by the cation, been larger when the ionic interaction is stronger.[85] In solid Na-AOT the splitting has a value of 28 cm^{-1} and, in RMs at $W_0 = 0$ the band shows the doublet at 1255 cm^{-1} and 1213 cm^{-1} with $\Delta\nu_{asym}SO_3$ value of 42 cm^{-1} in the benzene RMs which reflects an increase in the strength between Na^+ - SO_3^- interaction.[80,85,88b] In presence of water entrapped the magnitude of the $\Delta\nu_{asym}SO_3$ value decreases with increasing the micelle hydration due to a weakening of the sodium-sulfonate interaction after hydrogen bond interaction between water and the AOT polar head group with the corresponding increases in their spatial separation.[80]

In Figure 4 A, it is shown the FT-IR spectra of bmim-AOT in chlorobenzene at different W_0 values in the region of the asymmetric stretching mode of SO_3^-. In Figure 4 B, is presented the splitting of the AOT's asymmetric S=O stretching band frequency ($\Delta\nu_{asym}SO_3$) upon increasing W_0 in both RMs explored. In the Supporting information, for comparison, Figure S2 is included where are plotted the FT-IR spectra corresponding to Na-AOT in chlorobenzene at different W_0 values.

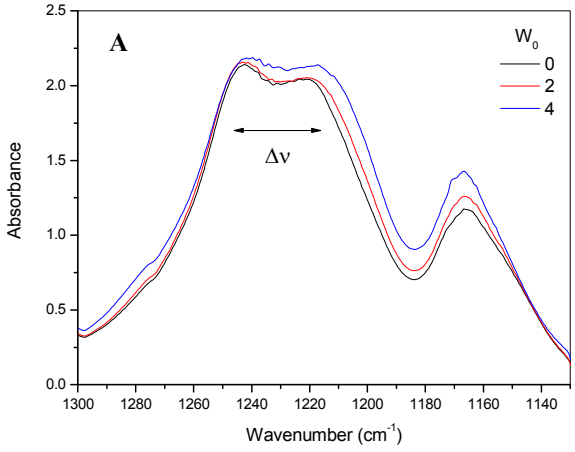

View Article Online
DOI: 10.1039/C5SM02421H

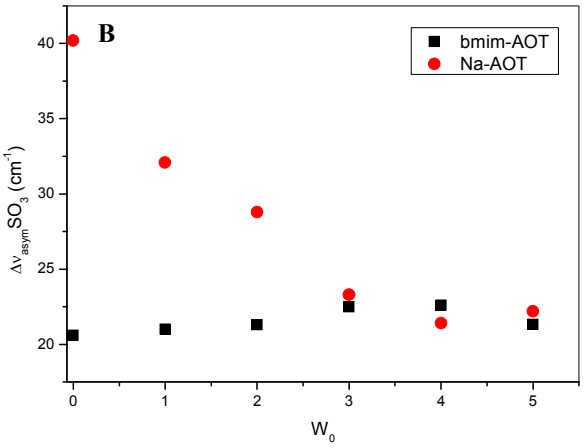

Figure 4. A) FT-IR spectra of chlorobenzene/bmim-AOT/water RMs at different W_0 values in the region of 1300-1130 cm^{-1}. The chlorobenzene bands have been subtracted. [bmim-AOT] = 0.05 M. B) Splitting of the asymmetric S=O stretching band frequency ($\Delta\nu_{asym}SO_3$) upon increasing W_0 in different chlorobenzene/surfactant/water RMs. Na-AOT (○) and bmim-AOT (■). [Surfactant] = 0.05 M.

At $W_0 = 0$, it can be seen that the splitting of the $\nu_{asym}SO_3$ band decreases from 40 cm^{-1} in Na-AOT RMs to 20 cm^{-1} in bmim-AOT RMs. These changes indicate a weaker SO_3^--$bmim^+$ interaction in comparison with the SO_3^--Na^+ interaction.

When the water content is increased, it is possible to observe that the shape of the band in bmim-AOT RMs does not show any significant change in its position, shape or intensity. Moreover, the magnitude of the band splitting remained practically constant as the W_0 was increased (Figure 4 B). These results are very different to those obtained for water entrapped in Na-AOT RMs (see circles in Figure 4 B), in which the magnitude of the $\Delta\nu_{asym}SO_3$ values decreases as a consequence of the interaction between the water molecules and the surfactant polar head group at the interface.[30,87,88b] In bmim-AOT RMs, the absence of variation in the asymmetric sulfonate band ($\Delta\nu_{asym}SO_3 \approx 21$ cm^{-1}) suggests that water molecules do not considerably disrupt the weak interaction between the SO_3^- and $bmim^+$ since both ions (SO_3^- - $bmim^+$) are spatially distant from

View Article Online
DOI: 10.1039/C5SM02421H

each other even at $W_0 = 0$. However, the absence of changes of this band with the water content cannot be interpreted as water-polar head interaction.

Other interesting fact to note in Figure 4 A is that in bmim-AOT RMs there is a band around 1166 cm^{-1}, which is attributed to a combination of C-O and C-C stretching modes of the ester groups of AOT moiety.[88b] In Na-AOT RMs, these stretching appear as a shoulder of the asymmetric sulfonate band because the vicinity of sulfonate groups hides these modes.[85] Thus, we conclude that the presence of the band at 1166 cm^{-1} in bmim-AOT RMs indicates that the sulfonate groups are more distant to each other than in Na-AOT, probably due to the location of $bmim^+$ near to the interface in comparison with Na^+.

Sulfonate symmetric stretching band ($\nu_{sym}SO_3$)

Figures S3 A and B, from the Supporting Information section, show the FT-IR spectra of bmim-AOT in chlorobenzene at different W_0 values in the region of the symmetric stretching mode of SO_3^-. Figure 5 shows the shifting of the $\nu_{sym}SO_3$ for both surfactants upon increasing the W_0 value.

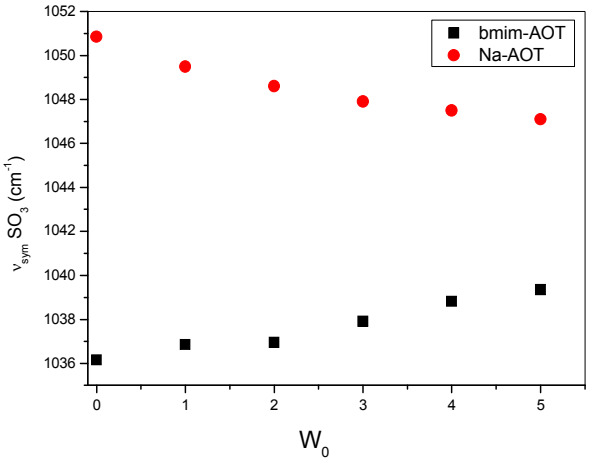

Figure 5. Shifts of the symmetric S=O stretching band ($\nu_{sym}SO_3$) upon increases W_0 for the (■) benzene/bmim-AOT/water and (●) benzene/Na-AOT/water RMs. [Surfactant] = 0.05 M.

View Article Online
DOI: 10.1039/C5SM02421H

From the results presented in Figure 5 it is important to note two facts: i) the shift observed increasing the W_0 is opposite in both RMs and, ii) the $\nu_{sym}SO_3$ values at $W_0 = 0$ are clearly different for bmim-AOT (1036 cm^{-1}) than for Na-AOT (1050 cm^{-1}).

It is known that the addition of water to the Na-AOT RMs system, causes a shift in the $\nu_{sym}SO_3$ value to lower frequencies[80,85], in our case from 1050 to 1047 cm^{-1} when the W_0 values increased from 0 to 5 (Figure 5). This shift has been attributed to hydrogen bond interactions between the water molecules and the SO_3^- group of AOT.[80] Also, the hydrogen bond weakens the electrostatic Na-SO_3 interaction, which is also affected by ion-dipole interactions between water and the sodium counterion.[80] The differences in the $\nu_{sym}SO_3$ values observed for bmim-AOT and Na-AOT at $W_0 = 0$ and the shift to higher frequencies in bmim-AOT RMs when the water content increases can be explained considering the size of the cation and the weakness of the interaction with the SO_3^- group previously discussed. In this sense, Moran et al.[88b] studied the effect of replacing the AOT counterions for different alkali-metal and they found that, for example, for Na^+ the symmetrical mode was observed at 1050 cm^{-1} and for Cs^+ at 1043 cm^{-1}. The authors explained these results taking into account that the increment in the cation size, reduce the positive charge density decreasing the interaction between the cation and the SO_3^- group. Oshitani et al.[35] in a work where H-AOT surfactant (AOT with H^+ as counterion[91]) was used to create isooctane/H-AOT/water microemulsion, showed that the $\nu_{sym}SO_3$ values increases from 1038 cm^{-1} in H-AOT to 1044-1046 cm^{-1} when the H^+ counterion was replaced by different alkali-metal cations. The increase in $\nu_{sym}SO_3$ values was attributed again to a strengthening of the interactions between counterions and the polar headgroup. Herein, as the positive charge is delocalized in the $bmim^+$ ion[92] (see Scheme 1) while it is not in the small Na^+, we expect a stronger interaction between SO_3^- and Na^+ than with $bmim^+$ cation.[75] Thus, we suggest that the replacement of Na^+ for a more voluminous cation (with more delocalized positive charge) is the cause for the reduction of the interaction cation-SO_3 and consequently affect the symmetrical sulfonate stretching mode. The addition of water, which interact with the SO_3^- group (as it was showed in the O-D stretching mode data), can reduce the

View Article Online
DOI: 10.1039/C5SM02421H

delocalization of negative charge on the O of the SO_3^- group increasing the frequency of the symmetrical mode.[78]

$bmim^+$ C-H stretching band (ν_{C-H})

For the ILs composed of 1-alkyl-3-methyl imidazolium, the infrared peaks found between 3200 and 3100 cm^{-1} are assigned to the aromatic C-H stretching modes of C(2)-H and C(4,5)-H on the imidazolium cation (Scheme 1).[74,75,93,94] The band at lower frequency is assigned to the C(2)-H stretching modes because the group has a larger positive charge density than the C(4,5)-H groups, which leads to smaller force constants.[78] These stretching vibrations modes in $bmim^+$ can be used to evaluate the cation-anion interactions in complex systems such as RMs[74,75] since $bmim^+$ interacting strongly with anions can diminish its positive charge density with the consequent decrease in the ν_{C-H} values.[78]

Figure S4 shows the FT-IR spectra of bmim-AOT in chlorobenzene at different W_0 values, in the region of 3200-3100 cm^{-1}. Shifts of both stretching frequencies upon increases W_0 in bmim-AOT RMs are plotted in Figure 6. The results show that both stretching modes shift to higher frequencies when the water content increases. For example, at $W_0 = 0$ the $\nu_{C(2)-H}$ and $\nu_{C(4,5)-H}$ appear at 3105 cm^{-1} and 3145 cm^{-1}, respectively. When the water content increase until $W_0 = 5$, the $\nu_{C(2)-H}$ and $\nu_{C(4,5)-H}$ shift to 3112 cm^{-1} and 3151 cm^{-1}.

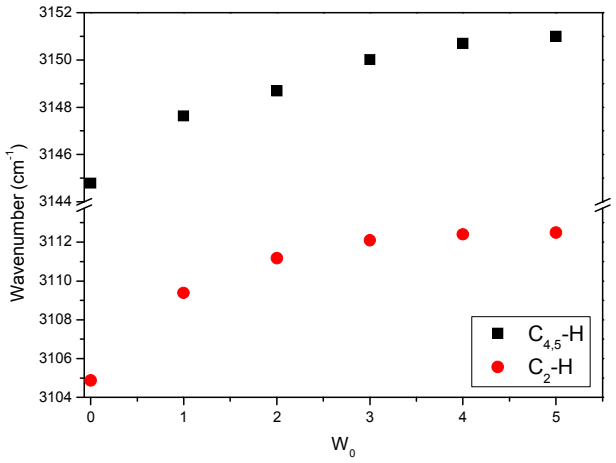

View Article Online
DOI: 10.1039/C5SM02421H

Figure 6. Shift of the C(2)-H and C(4,5)-H stretching frequencies of $bmim^+$ upon increase of W_0 in chlorobenzene/bmim-AOT/water RMs: (●) C(2)-H and (■) C(4,5)-H. [bmim-AOT] = 0.05 M.

The variation in the observed values of the C-H vibration modes, are evidences of an important perturbation on the $bmim^+$ microenvironment when water is added to the RMs. As discussed before at $W_0 = 0$, there is a weak electrostatic interaction between $bmim^+$ and SO_3^-, which is altered on addition of water molecules. In this sense, we suggest that water through its free electron pairs solvates the positive charge of $bmim^+$ through ion-dipole interaction. Thus, when water is added to the bmim-AOT RMs, the initial $bmim^+$-SO_3^- interaction at $W_0 = 0$ is replaced by water (electron pair)-$bmim^+$ and water (hydrogen bond)-SO_3^-. Thus, since water (electron pair)-$bmim^+$ is weaker than the electrostatic interaction $bmim^+$-SO_3^-, the positive charge density on $bmim^+$ shifting the C-H vibrations modes to high frequencies. A consequence of these implies that water molecules have less electron donor capacity at the interface than the corresponding in Na-AOT RMs.

V. ^1H NMR experiments

Figure S5 A and B, displays typical ^1H NMR spectra for water entrapped in benzene/bmim-AOT RMs at different W_0 in the region of 9.5-8.9 and 4.7-3.3 ppm, respectively. Different protons can be investigated and first we present the results obtained sensing the H of the water entrapped and, then the protons nearest to the polar head group in bmim-AOT surfactant (protons I and I´ of AOT and, 2 of $bmim^+$ in Scheme 1).

Water`s protons

In Figure 7, is shown the data corresponding to the chemical shift of H (from water) in the bmim-AOT RMs varying the water content. As it can be seen, the water`s proton signal shifts downfield when W_0 is increased. Thus, the proton from water molecules change from 3.79 ppm at $W_0 = 2$ up to 4.26 at $W_0 = 4.5$. It should be noted that in the bmim-AOT RMs the value of H for

View Article Online
DOI: 10.1039/C5SM02421H

neat water[95] (4.85 ppm) was not achieved (see straight line in Figure 7). This upfield shift of the proton signal (from water) in the RMs in comparison with neat water was observed previously by Heatley[95] in C_6D_6/Na-AOT/water RMs, and by Stahla et al.[96] in the C_6D_{12}/Na-AOT/water system. In both cases, the shift was attributed to the entrapped water having its hydrogen bond structure disrupted due to its interaction with the surfactant. With the increasing of the amount of water within the RMs, it begins to recover the hydrogen bond structure of neat water and the proton signal tends to the neat one value. The interaction between the entrapped water and the interface leads to a less water molecules interacting with itself and consequently a more upfield shift of the proton signal. As we suggest from the FT-IR studies, also in our system the interaction of the entrapped water and the interface disrupt its hydrogen-bond structure.

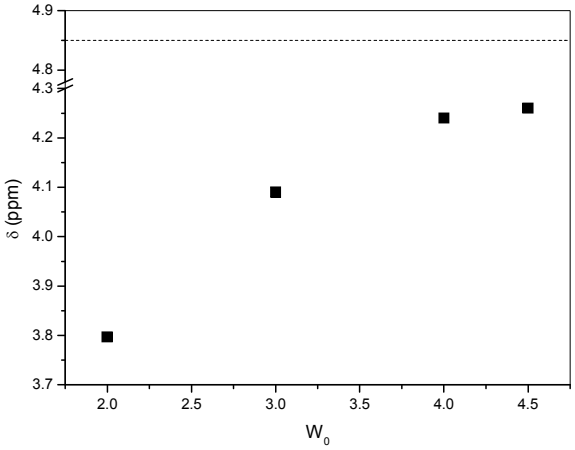

Figure 7. ^{1}H NMR chemical shifts of H (from water) benzene/bmim-AOT/water RMs at different W_0. [bmim-AOT] = 0.05 M. The corresponding value for neat water (**- - -**) is included to comparison.

Surfactant`s protons

The surfactant's protons[74,75,95-97] also can be used as a probe to study the microenvironment created in the bmim-AOT RMs (See Scheme 1). Figure 8 shows the chemical shifts of the H1 protons associated with the anion AOT in bmim-AOT RMs varying the water content. Figure S6

View Article Online
DOI: 10.1039/C5SM02421H

shows the AOT´s H1` chemical shift for the same system. As it can be observed, both signals showed upfield shift when the $W_0$ increases. For example, the signal assigned to H1 appears at 4.62 ppm at $W_0$ = 0 and shift to 4.52 ppm at $W_0$ = 4.5, while the H1` signal appears at 3.58 ppm in absence of water and shift to 3.49 ppm at W_0 = 4.5. On the other hand, the behavior of the protons corresponding to the polar head group of Na-AOT was explored in the past. For example, Heatley[95] reported that in the systems C_6D_6/Na-AOT/water the signal assigned to the H1 proton shift from 4.86 ppm at W_0 = 1.0 up to 4.67 ppm at W_0 = 5.3, while H1´ shift from 3.64 to 3.55 ppm in the same range of W_0. This behavior was attributed to the increasing spatial separation between anion AOT and its counterion, which occurs as a consequence of the hydrogen bond interaction between the sulfonate group and the entrapped water. Stahla et al.[96] studied the ^{1}H NMR signals assigned to the anion AOT polar head with different metal counterions. They observed that increasing the counterion sizes the signals of the protons nearest to the sulfonate group shifted upfield due to a reduction of the interaction between the metal and the anionic moiety. Consequently, since as we have already explained, in bmim-AOT there is a weaker interaction between SO_3^- and $bmim^+$ than that observed for SO_3^- and sodium, which is reflected in the different chemical shift values observed for the protons of the AOT moiety.

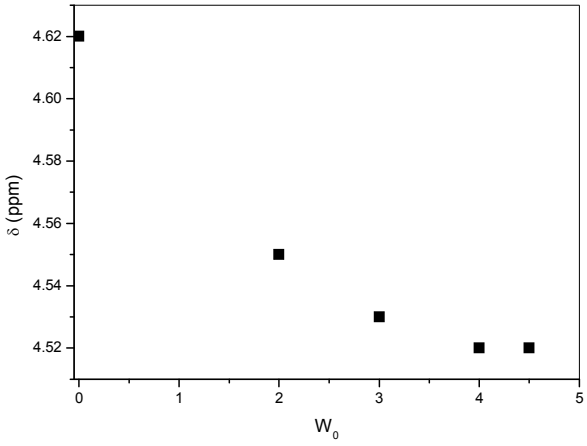

Figure 8. ^{1}H NMR chemical shifts of AOT H1 in benzene/bmim-AOT/water RMs at different W_0.

View Article Online
DOI: 10.1039/C5SM02421H

[bmim-AOT] = 0.05 M.

The presence of H atoms in $bmim^+$ makes possible to monitor the microenvironment of this part of the surfactant. Figure 9 shows the ^1H NMR chemical shift of the H2 (see Scheme 1) signal for $bmim^+$ cation in the bmim-AOT RMs, studied at different W_0. We focus on the peak associated with this proton because it is particularly sensitive to the environment.[53,74,75,97,98] The peak positions of the H2 showed an upfield shift as W_0 was increased, moving from 9.33 ppm at W_0 = 0 to 9.16 at W_0 = 4.5. This shift of the H2 signal observed for bmim-AOT RMs could be attributed to water interacting with the $bmim^+$. As we have explained before, in the bmim-AOT RMs the hydrogen bond structure of the entrapped water is disrupted due to the interaction with the interface. The results obtained for the H2 signal indicate that the $bmim^+$ interacts with the entrapped water as it was suggested by FT-IR.

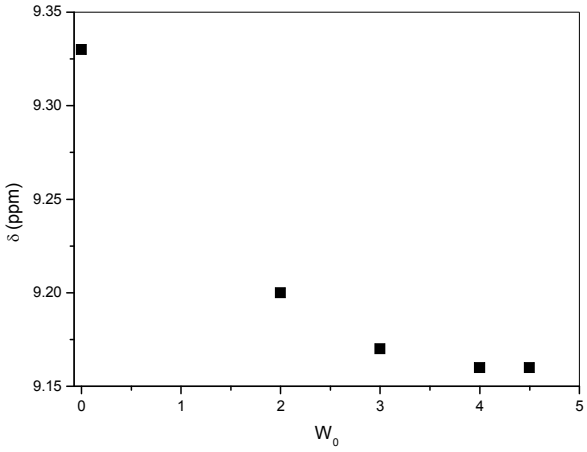

Figure 9. ^1H NMR chemical shifts of $bmim^+$ H2 in benzene/bmim-AOT/water RMs at different W_0. [bmim-AOT] = 0.05 M.

Thus, taking into account all the results obtained, the bmim-AOT surfactant location and the water-surfactant interaction at the RMs interface allow us to propose the schematic representation shown in Scheme 2A. We want to highlight that a new interface is created with different physicochemical

View Article Online
DOI: 10.1039/C5SM02421H

properties than Na-AOT (Scheme 2B).

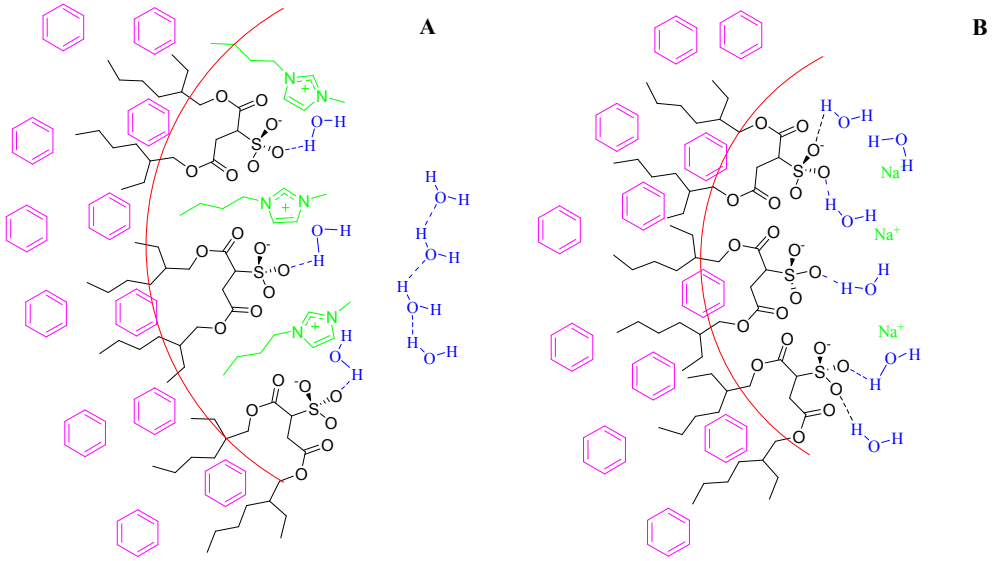

Scheme 2. Schematic representation of surfactants (A: bmim-AOT and B: Na-AOT) and water molecules location at the interface in benzene/surfactant/water RMs.

CONCLUSIONS

In the present work we showed how the water properties at the interface of RMs can be modified using a novel IL like-surfactant such as bmim-AOT. Particularly, in the aromatic solvent/bmim-AOT/water RMs investigated, DLS and SLS reveal the formation of RMs and that water interacts with the RMs interface since the droplet sizes values increase as the W_0 values increases. Furthermore, it is shown that the RMs consist of discrete spherical and non-interacting droplets of water stabilized by the bmim-AOT surfactant. To the best of our knowledge this is the first report where bmim-AOT RMs uses only water as polar component. From FT-IR and ^{1}H NMR data if bmim-AOT and Na-AOT are compared, a difference in the magnitude of the water-surfactant interaction at the interface is observed. For the bmim-AOT RMs a weaker water-surfactant interaction can be invoked in comparison with the RMs created by Na-AOT. This leads to less water molecules interacting with the interface in bmim-AOT RMs, with its hydrogen bond

View Article Online
DOI: 10.1039/C5SM02421H

network not completely disrupted (Scheme 2A). These results are interesting since a simple change in the cationic component in the surfactant, promotes remarkable changes in the RMs interface, for example modifying the hydrogen bond ability of the water at the interface.

EXPERIMENTAL SECTION

Materials

Sodium 1,4-bis-2-ethylhexylsulfosuccinate (Na-AOT), from Sigma (> 99% purity) was used as received and dried under vacuum prior use. Ultrapure water was obtained from Labonco equipment model 90901-01. D_2O, benzene, *n*-heptane, chlorobenzene and dichloromethane from Sigma (HPLC quality), were used without prior purification. 1-butyl-3-methylimidazolium chloride (bmimCl) from Sigma (> 97 % purity) was recrystallized according procedure descripted in reference 99.

bmim-AOT preparation: The IL-like surfactants used, 1-butyl-3-methylimidazolium 1,4-bis-2-ethylhexylsulfosuccinate (bmim-AOT, Scheme 1) was obtained according the experimental procedure descripted in reference 51. Thus, to obtain bmim-AOT the mixture of Na-AOT/dichloromethane and bmimCl/dichloromethane solutions (containing equimolar fractions of both reactants) were combined in a round-bottom flask and stirred at room temperature for 72 hours. During the stirring, a white precipitate appears and it was attributed to NaCl formation. The majority of NaCl was removed from the dichloromethane solution by centrifugation. After that the dichloromethane solution containing bmim-AOT was washed with small amounts of water until the aqueous fraction was free of chloride ion ($AgNO_3$ test). Once the NaCl was eliminated, the dichloromethane was removed by vacuum evaporation. The IL (bmim-AOT) thus obtained was colorless and highly viscous liquid, as we previously reported.[51] The formation of bmim-AOT was confirmed by ^{1}H NMR technique. Figure S7 show that all protons corresponding to the anionic (AOT) and to cationic ($bmim^+$) components are present. The chemical shifts values of the most important H of bmim-AOT obtained in $CDCl_3$ are included in Table S2.

View Article Online
DOI: 10.1039/C5SM02421H

Prior to use, bmim-AOT was dried under vacuum for 4 hours.

Methods

RMs preparation: The stock solutions of bmim-AOT in benzene (or chlorobenzene) were prepared by mass and volumetric dilution. Aliquots of these stock solutions were used to make individual reverse micelle solutions with different amount of water, defined as W_0 = [water] / [surfactant]. The incorporation of water into each micellar solutions were performed using calibrated microsyringes. To obtain optically clear solutions they were shaken in a sonicating bath. The resulting solutions were clear solutions with a single phase. The W_0 was varied between 0-6 for bmim-AOT RMs. It was not possible to obtain higher values of W_0 due to turbidity problems. The lowest value for W_0 ($W_0 = 0$), corresponds to a system without water addition. In the DLS, SLS and NMR experiments the surfactant concentration was keep constant and equal to 0.05 M. For the FT-IR experiments two different surfactant concentrations (0.05 and 0.2 M) were used.

To evaluate the amount of water (W_0^{max}) able to be dispersed in the systems investigated, we prepared stock solutions of different surfactant concentration (0.02, 0.05, 0.1 and 0.2 M) in the nonpolar solvents (*n*-heptane, chlorobenzene and benzene) and added water to the samples. The maximum W_0 values reached (W_0^{max}) for bmim-AOT were independent of the surfactant concentration.

General

The apparent diameters of the different bmim-AOT RMs were determined by dynamic light scattering (DLS, Malvern 4700 with goniometer) with an argon-ion laser operating at 488 nm. Cleanliness of the cuvettes used for measurements was of crucial importance for obtaining reliable and reproducible data.[100] Cuvettes were washed with ethanol, and then with doubly distilled water and dried with acetone. Prior to use the samples were filtered three times using an Acrodisc with 0.2 μm PTFE membrane (Sigma) to avoid dust or particles presents in the original solution. Before introducing each sample to the cuvette, it was rinsed with pure benzene twice, then with the surfactant stock solution, and finally with the sample to be analyzed. Prior making measurements on

View Article Online
DOI: 10.1039/C5SM02421H

a given day, the background signals from air and benzene were collected to confirm cleanliness of the cuvettes. Prior to data acquisition, the samples were equilibrated in the DLS instrument for 10 min at 25 ºC. To obtain valid results from DLS measurements requires knowledge of the system refractive index and viscosity in addition to well-defined conditions. Since we worked with dilute solutions, the refractive indices and viscosities for the RM solutions were assumed to be the same as neat benzene.[101] Multiple samples at each size were made, and thirty independent size measurements were made for each individual sample at the scattering angle of 90º. The instrument was calibrated before and during the course of experiments using several different size standards. Thus, we are confident that the magnitudes obtained by DLS measurements can be taken as statistically meaningful for all the systems investigated. The algorithm used was CONTIN and the DLS experiments shown that the polidispersity of the RMs were less than 5 %.

The aggregation numbers (N_{agg}) of the bmim-AOT and Na-AOT RMs were determined by static light scattering (SLS) technique in the same equipment that the one used in DLS. All the measurements were made at an angle of 90º and Debye plots were created using solutions with different surfactant concentration at fixed W_0 for all the RMs studied (See Figure S8). From the SLS experiments, the weight-averaged molar masses were determined and the N_{agg} values for all the systems investigated were calculated according the procedure detailed in literature[102] (See Table S3). In order to obtain the *dn/dc* values (data required for the SLS measurements) a differential refractometer was used (Brookhaven Instruments Corporation, BI-DNDCW model) with a tungsten lamp operating at 470 nm.

FT-IR spectra were recorded with a Nicolet IMPACT400 FT-IR spectrometer. IR cell of the type Irtran-2 (0.5 mm of path length) from Wilmad Glass (Buena, NJ) was used. FT-IR spectra were obtained by co-adding 200 spectra at a resolution of 0.5 cm^{-1}. For the experiments performed on the aromatic C-H, C=O, asymmetric and symmetric SO_3^- stretching modes, the benzene (or chlorobenzene) spectrum was used as the background. For the O-D stretching band a different procedure was performed. The ν_{OD} spectral band of HOD was superimposed on a finite background.

View Article Online
DOI: 10.1039/C5SM02421H

It was assumed that this background could be approximated with the spectrum of 100% H_2O in the ν_{OD} spectral region.[81,82,89] Therefore the reference sample, at each W_0 values, was a surfactant solution containing exactly the same W_0 but adjusted with pure water. The reason for using partially deuterated water was explained in the results and discussion section.

For the ^1H NMR experiments a Bruker 400 NMR spectrometer was used. The spectra were recorded at a digital resolution of 0.06 Hz/data point. The spectrometer probe temperature, 25 $^{\circ}C$, was periodically monitored by measuring the chemical shift difference values between the two singlets of a methanol reference sample which is well-known that depends on the temperature.[70] The probe thermal stability was assured by the observation that successive measurements of the sample chemical shift (after 10 minutes in the probe for thermal equilibration) were within digital resolution limit. For the study in RMs, a capillary tube containing D_2O was introduced in the NMR tube and was used as a frequency "lock". Chemical shifts were measured relative to internal TMS and the values were reproducible within 0.01 ppm. All NMR data were processed using MestReC 4.8.6 for window and plotted and fitted using Microcal OriginPro 7.

ELECTRONIC SUPPLEMENTARY INFORMATION AVAILABLE: Table S1: Apparent diameter (d_{app}) and polydispersity index (PDI) values of benzene/bmim-AOT/water RMs varying W_0; Table S2: ^1H NMR chemical shifts (in ppm) for bmim-AOT and Na-AOT surfactants in Cl_3CD; Table S3: *dn/dc*, Micellar molecular weight (M_W) and aggregation numbers (N_{agg}) values of benzene/bmim-AOT/water and benzene/Na-AOT/water RMs obtained varying the surfactant concentration at W_0 = 5; Figure S1: FT-IR spectra of benzene/surfactant/HDO RMs at different W_0 values in the region of 2640-2420 cm^{-1}; Figure S2: FT-IR spectra of chlorobenzene/Na-AOT/water RMs at different W_0 values in the region of 1300-1140 cm^{-1}; Figure S3: FT-IR spectra of chlorobenzene/surfactant/water RMs at different W_0 values in the region of symmetrical sulfonate mode. (A) bmim-AOT and (B) Na-AOT; Figure S4: FT-IR spectra of $bmim^+$ in chlorobenzene/bmim-AOT RMs at different W_0 values, in the region of 3200-3100 cm^{-1}; Figure S5: Typical ^1H NMR spectra for benzene/bmim-

View Article Online
DOI: 10.1039/C5SM02421H

AOT RMs at different W_0 in the region of 9.5-8.9 ppm (A) and 4.7-3.3 ppm (B); Figure S6: ^{1}H NMR chemical shifts of AOT H1` in benzene/bmim-AOT/water RMs at different W_0; Figure S7: ^{1}H NMR spectrum of bmim-AOT in Cl_3CD; and Figure S8: Debye plots of K^*C/R_θ in benzene/surfactant/water RMs as a function of the surfactant concentration (C) obtained by SLS at 90° scattering angle, are available free of charge.

ACKNOWLEDGEMENTS

We gratefully acknowledge the financial support for this work by the Consejo Nacional de Investigaciones Científicas y Técnicas (CONICET), Agencia Nacional de Promoción Científica y Técnica and Secretaría de Ciencia y Técnica de la Universidad Nacional de Río Cuarto. J.J.S., N.M.C. and R.D.F. hold a research position at CONICET. C.M.O.L. thanks CONICET for a research fellowship.

NOTES AND REFERENCES

1 (a) T. Welton, Ionic Liquids in Green Chemistry. *Green Chem.* 2011, **13**, 225-225; (b) J. P. Hallett, T. Welton, Room-Temperature Ionic Liquids: Solvents for Synthesis and Catalysis. 2. *Chem. Rev.* 2011, **111**, 3508–3576; (c) T. Welton, P. Wasserscheid, *Ionic Liquids in Synthesis*, VCH-Wiley, Weinheim, 2002.

2 (a) Z. Yan, C. Dai, M. Zhao, Y. Li, M. Du, D. Peng, Study of pH-Responsive Surface Active Ionic Liquids: The Formation of Spherical and Wormlike Micelles. *Colloid Polym. Sci.* 2015, **293**, 1759–1766; (b) N. Cheng, P. Yu, T. Wang, X. Sheng, Y. Bi, Y. Gong, L. Yu, Self-Aggregation of New Alkylcarboxylate-Based Anionic Surface Active Ionic Liquids: Experimental and Theoretical Investigations. *J. Phys. Chem. B* 2014, **118**, 2758–2768; (c) C. Cao, J. Lei, T. Huang, F.-P. Du, Impact of Ionic Liquid-Type Imidazolium Surfactant Addition on Dynamic Properties of BSA Adsorption Layers at Different pH. *Soft Matter* 2014, **10**, 8896–8904; (d) H. Yan, Y. Long, K. Song, C.-H. Tung, L. Zheng, Photo-Induced Transformation from Wormlike to Spherical Micelles

View Article Online
DOI: 10.1039/C5SM02421H

Based on Pyrrolidinium Ionic Liquids. *Soft Matter* 2013, **10**, 115–121; (e) K. S. Rao, P. S. Gehlot, T. J. Trivedi, A. Kumar, Self-Assembly of New Surface Active Ionic Liquids Based on Aerosol-OT in Aqueous Media. *J. Colloid Interface Sci.* 2014, **428**, 267–275; (f) F. Comelles, I. Ribosa, J. J. González, M. Garcia, Micellization of Sodium Lauryl Ether Sulphate (SLES) and Short Chain Imidazolium Ionic Liquids in Aqueous Solution. *J. Colloid Interface Sci.* 2014, **425**, 44–51.

3 (a) Y. Zhao, X. Chen, B. Jing, X. Wang, F. Ma, Novel Gel Phase Formed by Mixing a Cationic Surfactive Ionic Liquid C_{16}mimCl and an Anionic Surfactant SDS in Aqueous Solution. *J. Phys. Chem. B* 2009, **113**, 983–988; (b) F. Geng, J. Liu, L. Zheng, L. Yu, Z. Li, G. Li, C. Tung, Micelle Formation of Long-Chain Imidazolium Ionic Liquids in Aqueous Solution Measured by Isothermal Titration Microcalorimetry. *J. Chem. Eng. Data* 2010, **55**, 147–151.

4 C. C. Villa, F. Moyano, M. Ceolin, J. J. Silber, R. D. Falcone, N. M. Correa, A Unique Ionic Liquid with Amphiphilic Properties That Can Form Reverse Micelles and Spontaneous Unilamellar Vesicles. *Chem. - A Eur. J.* 2012, **18**, 15598–15601.

5 C. C. Villa, J. J. Silber, N. M. Correa, R. D. Falcone, Effect of the Cationic Surfactant Moiety on the Structure of Water Entrapped in Two Catanionic Reverse Micelles Created from Ionic Liquid-Like Surfactants. *ChemPhysChem* 2014, **15**, 3097–3109.

6 O. Rojas, B. Tiersch, C. Rabe, R. Stehle, A. Hoell, B. Arlt, J. Koetz, Nonaqueous Microemulsions Based on N,N′-Alkylimidazolium Alkylsulfate Ionic Liquids. *Langmuir* 2013, **29**, 6833–6839.

7 T. L. Greaves, C. J. Drummond, Ionic Liquids as Amphiphile Self-Assembly Media. *Chem. Soc. Rev.* 2008, **37**, 1709–1726.

8 W. Kunz, T. Zemb, A. Harrar, Using Ionic Liquids to Formulate Microemulsions: Current State of Affairs. *Curr. Opin. Colloid Interface Sci.* 2012, **17**, 205–211.

9 O. Rojas, B. Tiersch, S. Frasca, U. Wollenberger, J. Koetz, A New Type of Microemulsion Consisting of Two Halogen-Free Ionic Liquids and One Oil Component. *Colloids Surfaces A Physicochem. Eng. Asp.* 2010, **369**, 82–87.

10 J. J. Silber, M. A. Biasutti, E. Abuin, E. Lissi, Interactions of Small Molecules with Reverse

View Article Online
DOI: 10.1039/C5SM02421H

Micelles. *Adv. Colloid Interface Sci.* 1999, **82**, 189–252.

11 N. M. Correa, J. J. Silber, R. E. Riter, N. E. Levinger, Nonaqueous Polar Solvents in Reverse Micelle Systems. *Chem. Rev.* 2012, **112**, 4569–4602.

12 J. Eastoe, G. Fragneto, B. H. Robinson, T. F. Towey, R. K. Heenan, F. J. Leng, Variation of Surfactant Counterion and Its Effect on the Structure and Properties of Aerosol-OT-Based Water-in-Oil Microemulsions. *J. Chem. Soc. Faraday Trans.* 1992, **88**, 461-471.

13 T. K. De, A. Maitra, Solution Behaviour of Aerosol OT in Non-Polar Solvents. *Adv. Colloid Interface Sci.* 1995, **59**, 95–193.

14 M. Hasegawa, T. Sugimura, Y. Suzaki, Y. Shindo, A. Kitahara, Microviscosity in Water Pool of Aerosol-OT Reversed Micelle Determined with Viscosity-Sensitive Fluorescence Probe, Auramine O, and Fluorescence Depolarization of Xanthene Dyes. *J. Phys. Chem.* 1994, **98**, 2120–2124.

15 I. R. Piletic, D. E. Moilanen, D. B. Spry, N. E. Levinger, M. D. Payer, Testing the Core/shell Model of Nanoconfined Water in Reverse Micelles Using Linear and Nonlinear IR Spectroscopy. *J. Phys. Chem. A* 2006, **110**, 4985–4999.

16 F. Moyano, S. S. Quintana, R. D. Falcone, J. J. Silber, N. M. Correa, Characterization of Multifunctional Reverse Micelles' Interfaces Using Hemicyanines as Molecular Probes. I. Effect of the Hemicyanines' Structure. *J. Phys. Chem. B* 2009, **113**, 4284–4292.

17 S. S. Quintana, F. Moyano, R. D. Falcone, J. J. Silber, N. M. Correa, Characterization of Multifunctional Reverse Micelles' Interfaces Using Hemicyanines as Molecular Probes. II: Effect of the Surfactant. *J. Phys. Chem. B* 2009, **113**, 6718–6724.

18 F. Moyano, R. D. Falcone, J. C. Mejuto, J. J. Silber, N. M. Correa, Cationic Reverse Micelles Create Water with Super Hydrogen-Bond-Donor Capacity for Enzymatic Catalysis: Hydrolysis of 2-Naphthyl Acetate by α-Chymotrypsin. *Chem. - A Eur. J.* 2010, **16**, 8887–8893.

19 A. M. Durantini, R. D. Falcone, J. J. Silber, N. M. Correa, A New Organized Media: Glycerol: N,N-Dimethylformamide mixtures/AOT/n- Heptane Reversed Micelles. The Effect of Confinement

View Article Online
DOI: 10.1039/C5SM02421H

on Preferential Solvation. *J. Phys. Chem. B* 2011, **115**, 5894–5902.

20 D. Blach, N. M. Correa, J. J. Silber, R. D. Falcone, Interfacial Water with Special Electron Donor Properties: Effect of Water-Surfactant Interaction in Confined Reversed Micellar Environments and Its Influence on the Coordination Chemistry of a Copper Complex. *J. Colloid Interface Sci.* 2011, **355**, 124–130.

21 F. M. Agazzi, R. D. Falcone, J. J. Silber, N. M. Correa, Solvent Blends Can Control Cationic Reversed Micellar Interdroplet Interactions. The Effect of n-heptane:Benzene Mixture on BHDC Reversed Micellar Interfacial Properties: Droplet Sizes and Micropolarity. *J. Phys. Chem. B* 2011, **115**, 12076–12084.

22 N. M. Correa, N. E. Levinger, What Can You Learn From a Molecular Probe? New Insights on the Behavior of C343 in Homogeneous Solutions and AOT Reverse Micelles. *J. Phys. Chem. B* 2006, **110**, 13050–13061.

23 S. S. Quintana, R. D. Falcone, J. J. Silber, N. M. Correa, Comparison between Two Anionic Reverse Micelle Interfaces: The Role of Water-Surfactant Interactions in Interfacial Properties. *ChemPhysChem* 2012, **13**, 115–123.

24 A. M. Durantini, R. D. Falcone, J. J. Silber, N. M. Correa, More Evidence on the Control of Reverse Micelles Sizes. Combination of Different Techniques as a Powerful Tool to Monitor AOT Reversed Micelles Properties. *J. Phys. Chem. B* 2013, **117**, 3818–3828.

25 P. A. Pieniazek, Y. Lin, J. Chowdhary, B. M. Ladanyi, J. L. Skinner, Vibrational Spectroscopy and Dynamics of Water Confined inside Reverse Micelles. *J. Phys. Chem. B* 2009, **113**, 15017–15028.

26 A. K. Satpati, M. Kumbhakar, S. Nath, H. Pal, Influence of Confined Water on the Photophysics of Dissolved Solutes in Reverse Micelles. *ChemPhysChem* 2009, **10**, 2966–2978.

27 O. A. El Seoud, Use of NMR to Probe the Structure of Water at Interfaces of Organized Assemblies. *J. Mol. Liq.* 1997, **72**, 85–103.

28 I. R. Piletic, H. S. Tan, M. D. Fayer, Dynamics of Nanoscopic Water: Vibrational Echo and

View Article Online
DOI: 10.1039/C5SM02421H

Infrared Pump-Probe Studies of Reverse Micelles. *J. Phys. Chem. B* 2005, **109**, 21273–21284.

29 M. Freda, G. Onori, A. Paciaroni, A. Santucci, Hydration and Dynamics of Aerosol OT Reverse Micelles. *J. Mol. Liq.* 2002, **101**, 55–68.

30 Q. Li, S. Weng, J. Wu, N. Zhou, Comparative Study on Structure of Solubilized Water in Reversed Micelles. 1. FT-IR Spectroscopic Evidence of Water/AOT/n-Heptane and Water/NaDEHP/n-Heptane Systems. *J. Phys. Chem. B* 1998, **102**, 3168–3174.

31 D. Cringus, A. Bakulin, J. Lindner, P. Vohringer, M. S. Pshenichnikov, D. A. Wiersma, Ultrafast Energy Transfer in Water-AOT Reverse Micelles. *J. Phys. Chem. B* 2007, **111**, 14193–14207.

32 A. Bumajdad, M. Madkour, E. Shaaban, O. A. El Seoud, FT-IR and 1H NMR Studies of the State of Solubilized Water in Water-in-Oil Microemulsions Stabilized by Mixtures of Single- and Double-Tailed Cationic Surfactants. *J. Colloid Interface Sci.* 2013, **393**, 210–218.

33 R. D. Falcone, M. A. Biasutti, N. M. Correa, J. J. Silber, E. Lissi, E. Abuin, Effect of the Addition of a Nonaqueous Polar Solvent (glycerol) on Enzymatic Catalysis in Reverse Micelles. Hydrolysis of 2-Naphthyl Acetate by α-Chymotrypsin. *Langmuir* 2004, **20**, 5732–5737.

34 J. A. Gutierrez, R. D. Falcone, M. A. Lopez-Quintela, D. Buceta, J. J. Silber, N. M. Correa, On the Investigation of the Droplet-Droplet Interactions of Sodium 1,4-bis(2-Ethylhexyl) Sulfosuccinate Reverse Micelles upon Changing the External Solvent Composition and Their Impact on Gold Nanoparticle Synthesis. *Eur. J. Inorg. Chem.* 2014, **12**, 2095–2102.

35 J. Oshitani, S. Takashina, M. Yoshida, K. Gotoh, Difference in Screening Effect of Alkali Metal Counterions on H-AOT-Based W/O Microemulsion Formation. *Langmuir* 2010, **26**, 2274–2278.

36 E. Bardez, N. Cao Vy, T. Zemb, Counterion-Driven Sphere to Cylinder Transition in Reverse Micelles: A Small Angle X-Ray Scattering and Conductometric Study. *Langmuir* 1996, **11**, 3374–3381.

37 C. M. Dunn, B. H. Robinson, F. J. Leng, Photon-Correlation Spectroscopy Applied to the Size Characterization of Water-in-Oil Microemulsion Systems Stabilized by Aerosol-OT; Effect of Change in Counterion. *Spectrochim. Acta Part A Mol. Spectrosc.* 1990, **46**, 1017–1025.

View Article Online
DOI: 10.1039/C5SM02421H

38 M. R. Harpham, B. M. Ladanyi, N. E. Levinger, The Effect of the Counterion on Water Mobility in Reverse Micelles Studied by Molecular Dynamics Simulations. *J. Phys. Chem. B* 2005, **109**, 16891–16900.

39 D. Fioretto, M. Freda, G. Onori, A. Santucci, Effect of Counterion Substitution on AOT-Based Micellar Systems: Dielectric Study of $Cu(AOT)_2$ Reverse Micelles in CCl_4. *J. Phys. Chem. B* 1999, **103**, 8216–8220.

40 J. Eastoe, T. F. Towey, B. H. Robinson, J. Williams, R. K. Heenan, Structures of Metal bis(2-Ethylhexylsulfosuccinate) Aggregates in Cyclohexane. *J. Phys. Chem.* 1993, **97**, 1459–1463.

41 A. Longo, G. Portale, W. Bras, F. Giannici, A. M. Ruggirello, V. T. Liveri, Structural Characterization of Frozen n-Heptane Solutions of Metal-Containing Reverse Micelles. *Langmuir* 2007, **23**, 11482–11487.

42 D. Fioretto, M. Freda, S. Mannaioli, G. Onori, A. Santucci, Infrared and Dielectric Study of $Ca(AOT)_2$ Reverse Micelles. *J. Phys. Chem. B* 1999, **103**, 2631–2635.

43 F. Caboi, G. Capuzzi, P. Baglioni, M. Monduzzi, Microstructure of Ca-AOT/Water/Decane W/O Microemulsions. *J. Phys. Chem. B* 1997, **101**, 10205-10212.

44 B. M. Ladanyi, Computer Simulation Studies of Counterion Effects on the Properties of Surfactant Systems. *Curr. Opin. Colloid Interface Sci.* 2013, **18**, 15–25.

45 R. Giordano, P. Migliardo, U. Wanderlingh, E. Bardez, C. Vasi, Structural Properties of Micellar Solutions. *J. Mol. Struct.* 1993, **296**, 265–269.

46 R. D. Falcone, N. M. Correa, N. E. Levinger, J. J. Silber, Ionic Liquids in soft confinement. Effect of the different Reverse Micelles interfaces on the entrapped Ionic Liquid structure. *Ionic Liquid-Based Surfactant Science: Formulation, Characterization, and Applications*, edited by B. K. Paul and S. P. Moulik. 2015. ISBN-10: 1118834194. ISBN-13: 9781118834190.

47 G. Revillod, N. Nishi, T. Kakiuchi, Orientation Correlation of Sulfosuccinate-Based Room-Temperature Ionic Liquids Studied by Polarization-Resolved Hyper-Rayleigh Scattering. *J. Phys. Chem. B* 2009, **113**, 15322–15326.

View Article Online
DOI: 10.1039/C5SM02421H

48 K. Lava, K. Binnemans, T. Cardinaels, Piperidinium, Piperazinium and Morpholinium Ionic Liquid Crystals. *J. Phys. Chem. B* 2009, **113**, 9506–9511.

49 N. Nishi, T. Kawakami, F. Shigematsu, M. Yamamoto, T. Kakiuchi, Fluorine-Free and Hydrophobic Room-Temperature Ionic Liquids, Tetraalkylammonium bis(2-Ethylhexyl)sulfosuccinates, and Their Ionic Liquid–water Two-Phase Properties. *Green Chem.* 2006, **8**, 349–355.

50 P. Brown, C. Butts, R. Dyer, J. Eastoe, I. Grillo, F. Guittard, S. Rogers, R. Heenan, Anionic Surfactants and Surfactant Ionic Liquids with Quaternary Ammonium Counterions. *Langmuir* 2011, **27**, 4563–4571.

51 P. Brown, C. P. Butts, J. Eastoe, D. Fermin, I. Grillo, H.-C. Lee, D. Parker, D. Plana, R. M. Richardson, Anionic Surfactant Ionic Liquids with 1-Butyl-3-Methyl-Imidazolium Cations: Characterization and Application. *Langmuir* 2012, **28**, 2502–2509.

52 P. Brown, C. P. Butts, J. Eastoe, I. Grillo, C. James, A. Khan, New Catanionic Surfactants with Ionic Liquid Properties. *J. Colloid Interface Sci.* 2013, **395**, 185–189.

53 T. Bai, R. Ge, Y. Gao, J. Chai, J. M. Slattery, The Effect of Water on the Microstructure and Properties of benzene/[bmim][AOT]/[bmim][BF_4] Microemulsions. *Phys. Chem. Chem. Phys.* 2013, **15**, 19301–19311.

54 N. Cheng, X. Ma, X. Sheng, T. Wang, R. Wang, J. Jiao, L. Yu, Aggregation Behavior of Anionic Surface Active Ionic Liquids with Double Hydrocarbon Chains in Aqueous Solution: Experimental and Theoretical Investigations. *Colloids Surfaces A Physicochem. Eng. Asp.* 2014, **453**, 53–61.

55 T. Yin, J. Wu, S. Wang, W. Shen, Structural Rearrangement in the Aqueous Solution of Surface Active Ionic Liquid 1-Butyl-3-Methylimidazolium bis(2-Ethylhexyl) Sulfosuccinate. *Soft Matter* 2015, **11**, 4717–4722.

56 V. G. Rao, S. Ghosh, C. Ghatak, S. Mandal, U. Brahmachari, N. Sarkar, Designing a New Strategy for the Formation of IL-in-Oil Microemulsions. *J. Phys. Chem. B* 2012, **116**, 2850–2855.

View Article Online
DOI: 10.1039/C5SM02421H

57 V. G. Rao, S. Mandal, S. Ghosh, C. Banerjee, N. Sarkar, Ionic Liquid-in-Oil Microemulsions Composed of Double Chain Surface Active Ionic Liquid as a Surfactant: Temperature Dependent Solvent and Rotational Relaxation Dynamics of Coumarin-153 in [Py][TF_2N]/[C_4mim][AOT]/benzene Microemulsions. *J. Phys. Chem. B* 2012, **116**, 8210–8221.

58 C. Banerjee, N. Kundu, S. Ghosh, S. Mandal, J. Kuchlyan, N. Sarkar, Fluorescence Resonance Energy Transfer in Microemulsions Composed of Tripled-Chain Surface Active Ionic Liquids, RTILs, and Biological Solvent: An Excitation Wavelength Dependence Study. *J. Phys. Chem. B* 2013, **117**, 9508–9517.

59 V. G. Rao, C. Banerjee, S. Ghosh, S. Mandal, J. Kuchlyan, N. Sarkar, A Step toward the Development of High-Temperature Stable Ionic Liquid-in-Oil Microemulsions Containing Double-Chain Anionic Surface Active Ionic Liquid. *J. Phys. Chem. B* 2013, **117**, 7472–7480.

60 V. G. Rao, S. Mandal, S. Ghosh, C. Banerjee, N. Sarkar, Phase Boundaries, Structural Characteristics, and NMR Spectra of Ionic Liquid-in-Oil Microemulsions Containing Double Chain Surface Active Ionic Liquid: A Comparative Study. *J. Phys. Chem. B* 2013, **117**, 1480–1493.

61 A. Khan E. Marques, Catanionic surfactants, in Specialists Surfactants, ed. I. D. Robb, Blackie Academic and Professional, Chapman & Hall, London, 1997, 37–80.

62 (a) S. K. Pal, A. H. Zewail, Dynamics of Water in Biological Recognition. *Chem. Rev.* 2004, **104**, 2099–2123; (b) R. Saha, S. Rakshit, P. K. Verma, R. K. Mitra, S. K. Pal, Protein–cofactor Binding and Ultrafast Electron Transfer in Riboflavin Binding Protein under the Spatial Confinement of Nanoscopic Reverse Micelles. *J. Mol. Recognit.* 2013, **26**, 59–66.

63 S. Rakshit, R. Saha, S. K. Pal, Modulation of Environmental Dynamics at the Active Site and Activity of an Enzyme under Nanoscopic Confinement: Subtilisin Carlsberg in Anionic AOT Reverse Micelle. *J. Phys. Chem. B* 2013, **117**, 11565–11574.

64 A. C. Fogarty, F. X. Coudert, A. Boutin, D. Laage, Reorientational Dynamics of Water Confined in Zeolites. *ChemPhysChem* 2014, **15**, 521–529.

65 M. A. López-Quintela, Synthesis of Nanomaterials in Microemulsions: Formation Mechanisms

View Article Online
DOI: 10.1039/C5SM02421H

and Growth Control. *Curr. Opin. Colloid Interface Sci.* 2003, **8**, 137–144.

66 R. A. Day, B. H. Robinson, J. H. R. Clarke, J. V. Doherty, Characterisation of Water-Containing Reversed Micelles by Viscosity and Dynamic Light Scattering Methods. *J. Chem. Soc. Faraday Trans. 1* 1979, **75**, 132-139.

67 N. M. Correa, D. H. Zorzan, L. D'Anteo, E. Lasta, M. Chiarini, G. Cerichelli, Reverse Micellar Aggregates: Effect on Ketone Reduction. 2. Surfactant Role. *J. Org. Chem.* 2004, **69**, 8231–8238.

68 R. D. Falcone, J. J. Silber, N. M. Correa, What Are the Factors That Control Non-aqueous/AOT/n-Heptane Reverse Micelle Sizes? A Dynamic Light Scattering Study. *Phys. Chem. Chem. Phys.* 2009, **11**, 11096–11100.

69 T. Liu, Y. Xie, B. Chu, Use of Block Copolymer Micelles on Formation of Hollow MoO_3 Nanospheres. *Langmuir* 2000, **16**, 9015–9022.

70 A. Salabat, J. Eastoe, K. J. Mutch, R. F. Tabor, Tuning Aggregation of Microemulsion Droplets and Silica Nanoparticles Using Solvent Mixtures. *J. Colloid Interface Sci.* 2008, **318**, 244–251.

71 A. Maitra, Determination of Size Parameters of Water Aerosol OT Oil Reverse Micelles From Their Nuclear Magnetic-Resonance Data. *J. Phys. Chem.* 1984, **88**, 5122–5125.

72 D. F. Evans, B. W. Ninham, Molecular Forces in the Self-Organization of Amphiphiles. *J. Phys. Chem.* 1986, **90**, 226–234.

73 Q. Li, T. Li, J. Wu, Electrical Conductivity of Water/Sodium Bis(2-Ethylhexyl) Sulfosuccinate/n-Heptane and Water/Sodium Bis(2-Ethylhexyl) Phosphate/n-Heptane Systems: The Influences of Water Content, Bis(2-Ethylhexyl) Phosphoric Acid, and Temperature. *J. Colloid Interface Sci.* 2001, **239**, 522–527.

74 D. D. Ferreyra, N. M. Correa, J. J. Silber, R. D. Falcone, The Effect of Different Interfaces and Confinement on the Structure of the Ionic Liquid 1-Butyl-3-Methylimidazolium Bis(trifluoromethylsulfonyl)imide Entrapped in Cationic and Anionic Reverse Micelles. *Phys. Chem. Chem. Phys.* 2012, **14**, 3460-3470.

View Article Online
DOI: 10.1039/C5SM02421H

75 D. Blach, J. J. Silber, N. M. Correa, R. D. Falcone, Electron Donor Ionic Liquids Entrapped in Anionic and Cationic Reverse Micelles. Effects of the Interface on the Ionic Liquid-Surfactant Interactions. *Phys. Chem. Chem. Phys.* 2013, **15**, 16746–16757.

76 S. Murgia, G. Palazzo, M. Mamusa, S. Lampis and M. Monduzzi, Aerosol-OT Forms Oil-in-Water Spherical Micelles in the Presence of the Ionic Liquid bmimBF_4. *J. Phys. Chem. B*, 2009, **113**, 9216–9225.

77 S. Murgia, G. Palazzo, M. Mamusa, S. Lampis, M. Monduzzi, Aerosol-OT in Water Forms Fully-Branched Cylindrical Direct Micelles in the Presence of the Ionic Liquid 1-Butyl-3-Methylimidazolium Bromide. *Phys. Chem. Chem. Phys.* 2011, **13**, 9238–9245.

78 R. M. Silverstein, F. X. Webster, D. J. Kiemle, *Spectrometric Identification of Organic Compounds*, J. Wiley, New York, 7th Ed. 2005.

79 W. F. Pacynko, J. Yarwood, G. J. T. Tiddy, Infrared and Far-Infrared Spectroscopic Studies on the Structure of Water in Lyotropic Liquid Crystals. *Liq. Cryst.* 1987, **2**, 201–214.

80 D. J. Christopher, J. Yarwood, P. S. Belton, B. P. A Hills, Fourier Transform Infrared Study of Water—head Group Interactions in Reversed Micelles Containing Sodium bis(2-Ethylhexyl) Sulfosuccinate (AOT). *J. Colloid Interface Sci.* 1992, **152**, 465–472.

81 L. P. Novaki, N. M. Correa, J. J. Silber, O. A. El Seoud, FTIR and 1H NMR Studies of the Solubilization of Pure and Aqueous 1,2-Ethanediol in the Reverse Aggregates of Aerosol-OT. *Langmuir* 2000, **16**, 5573–5578.

82 O. A. El Seoud, N. M. Correa, L. P. Novaki, Solubilization of Pure and Aqueous 1,2,3-Propanetriol by Reverse Aggregates of Aerosol-OT in Isooctane Probed by FTIR and 1H NMR Spectroscopy. *Langmuir* 2001, **17**, 1847–1852.

83 E. Odella, R. D. Falcone, J. J. Silber, N. M. Correa, How TOPO Affects the Interface of the Novel Mixed Water / AOT : TOPO / N -Heptane Reverse Micelles : Dynamic Light Scattering and Fourier Transform Infrared Spectroscopy Studies. *Phys. Chem. Chem. Phys.* 2014, **16**, 15457−15468.

View Article Online
DOI: 10.1039/C5SM02421H

84 M. Falk, On the Satellite Bands Accompanying the OH and OD Stretching Fundamentals of Isotopically Dilute HOO in Ice Ih. *J. Chem. Phys.* 1987, **87**, 28-30.

85 P. D. Moran, G. A. Bowmaker, R. P. Cooney, Vibrational Spectroscopic Study of the Structure of Sodium Bis(2-Ethylhexyl)sulfosuccinate Reverse Micelles and Water-in-Oil Microemulsions. *Langmuir* 1995, **11**, 738–743.

86 G. Calvaruso, A. Minore, V. T. Liveri, FT-IR Investigation of the Urea State in AOT Reversed Micelles. *J. Colloid Interface Sci.* 2001, **243**, 227–232.

87 A. M. Durantini, R. D. Falcone, J. J. Silber, N. M. Correa, Effect of the Constrained Environment on the Interactions between the Surfactant and Different Polar Solvents Encapsulated within AOT Reverse Micelles. *ChemPhysChem* 2009, **10**, 2034–2040.

88 (a) T. K. Jain, M. Varshney, A. Maitra, Structural Studies of Aerosol OT Reverse Micellar Aggregates by FT-IR Spectroscopy. *J. Phys. Chem.* 1989, **93**, 7409–7416; (b) P. D. Moran, G. A. Bowmaker, R. P. Cooney, J. R. Bartlett, J. L. Woolfrey, Vibrational Spectra of Metal Salts of bis(2-Ethylhexyl)sulfosuccinate (AOT). *J. Mater. Chem.* 1995, **5**, 295-302.

89 N. M. Correa, P. A. R. Pires, J. J. Silber, O. A. El Seoud, Real Structure of Formamide Entrapped by AOT Nonaqueous Reverse Micelles: FT-IR and1H NMR Studies. *J. Phys. Chem. B* 2005, **109**, 21209–21219.

90 H. Kise, K. Iwamoto, M. Seno, FT-IR Study of Micelle Formation of Ionic Surfactants and Water Solubilization in Nonpolar Organic Solvents. *Bull. Chem. Soc. Jpn.* 1982, **55**, 3856–3860.

91 E. Fernández, L. García-Río, P. Rodríguez-Dafonte, Degree of Counterion Binding on Water in Oil Microemulsions. *J. Colloid Interface Sci.* 2007, **316**, 1023–1026.

92 D. R. McFarlane, J. Sun, J. Golding, P. Meakin, M. Forsyth, High Conductivity Molten Salts Based on the Imide Ion. *Electrochim. Acta* 2000, **45**, 1271–1278.

93 J. C. Lassègues, J. Grondin, D. Cavagnat, P. Johansson, New Interpretation of the CH Stretching Vibrations in Imidazolium-Based Ionic Liquids. *J. Phys. Chem. A* 2009, **113**, 6419–6421.

94 (a) J. Shi, P. Wu, F. Yan, Further Investigation of the Intermolecular Interactions and

View Article Online
DOI: 10.1039/C5SM02421H

Component Distributions in a [Bmim][BF_4]-Based Polystyrene Composite Membranes Using Two-Dimensional Correlation Infrared Spectroscopy. *Langmuir* 2010, **26**, 11427–11434; (b) Q. G. Zhang, N. N. Wang, Z. W. Yu, The Hydrogen Bonding Interactions between the Ionic Liquid 1-Ethyl-3-Methylimidazolium Ethyl Sulfate and Water. *J. Phys. Chem. B* 2010, **114**, 4747–4754; (c) K. Noack, P. S. Schulz, N. Paape, J. Kiefer, P. Wasserscheid, A. Leipertz, The Role of the C2 Position in Interionic Interactions of Imidazolium Based Ionic Liquids: A Vibrational and NMR Spectroscopic Study. *Phys. Chem. Chem. Phys.* 2010, **12**, 14153–14161.

95 F. A Heatley, 1H Nuclear Magnetic Resonance Chemical-Shift Study of Inverted Microemulsions of Aerosol OT in Benzene and Cyclohexane. Partitioning of Water between Hydrocarbon and Aqueous Phases. *J. Chem. Soc. Faraday Trans. 1* 1988, **84**, 343-354.

96 M. L. Stahla, B. Baruah, D. M. James, M. D. Johnson, N. E. Levinger, D. C. Crans, 1H NMR Studies of Aerosol-OT Reverse Micelles with Alkali and Magnesium Counterions: Preparation and Analysis of MAOTs. *Langmuir* 2008, **24**, 6027–6035.

97 R. D. Falcone, B. Baruah, E. Gaidamauskas, C. D. Rithner, N. M. Correa, J. J. Silber, D. C. Crans, N. E. Levinger, Layered Structure of Room-Temperature Ionic Liquids in Microemulsions by Multinuclear NMR Spectroscopic Studies. *Chem. - A Eur. J.* 2011, **17**, 6837–6846.

98 A. D. Headley, N. M. Jackson, The Effect of the Anion on the Chemical Shifts of the Aromatic Hydrogen Atoms of Liquid 1-Butyl-3-Methylimidazolium Salts. *J. Phys. Org. Chem.* 2002, **15**, 52–55.

99 J. Dupont, P. A. Z. Suarez, C. S. Consorti, R. F. de Souza, Preparation of 1-Butyl-3-Methyl Imidazolium-Based Room Temperature Ionic Liquids. *Org. Synth.* 2002, **79**, 236-236.

100 M. A. Sedgwick, A. M. Trujillo, N. Hendricks, N. E. Levinger, D. C. Crans, Coexisting Aggregates in Mixed Aerosol OT and Cholesterol Microemulsions. *Langmuir* 2011, **27**, 948–954.

101 (a) J. P. Blitz, J. L. Fulton, R. D. Smith, Dynamic Light Scattering Measurements of Reverse Micelle Phases in Liquid and Supercritical Ethane. *J. Phys. Chem.* 1988, **92**, 2707–2710; (b) H. B. Bohidar, M. Behboudnia, Characterization of Reverse Micelles by Dynamic Light Scattering.

View Article Online
DOI: 10.1039/C5SM02421H

Colloids Surfaces A Physicochem. Eng. Asp. 2001, **178**, 313–323.

102 C. A. Gracia, S. Gómez-Barreiro, A. González-Pérez, J. Nimo, J. R. Rodríguez, Static and Dynamic Light-Scattering Studies on Micellar Solutions of Alkyldimethylbenzylammonium Chlorides. *J. Colloid Interface Sci.* 2004, **276**, 408–413.

View Article Online
DOI: 10.1039/C5SM02421H

TABLE OF CONTENTS (TOC)

How $bmim^+$ impact on the interaction between the entrapped water and the RM interface, modifying the interfacial water structure.